

TABLE III. Restrictions on the  $(L+1)/L$  amplitude ratio  $x$  for the  $\text{Ne}^{24}$  1.99  $\rightarrow$  0, 3.87  $\rightarrow$  1.99, and 4.76  $\rightarrow$  1.99 transitions.

Transition (MeV)	Spin of initial level	Restrictions on $x^a$
1.99 $\rightarrow$ 0	2	0
3.87 $\rightarrow$ 1.99	2	$-(0.15 \pm 0.15)$ , $-(2.1 \pm 0.6)^b$
4.76 $\rightarrow$ 1.99	1	no restrictions
4.76 $\rightarrow$ 1.99	2	$ x  > 4.3$ , $+(0.39 \pm 0.12)^b$

<sup>a</sup> One standard deviation.  
<sup>b</sup> Rejected at the 5% limit.

is most unlikely and reject it. The restrictions on the mixing ratio of the 4.76  $\rightarrow$  1.99 transition for spin assignments of 1 or 2 for the 4.76-MeV level are listed in Table III. The solution for  $J=2$  and  $x_{2.77} = +0.39$  barely reaches the 5% limit while the solution for  $|x| > 4.3$  requires an essentially pure quadrupole transition. We suggest that the most likely spin of the 4.76-MeV level is either  $J=0$  or 1.

#### IV. DISCUSSION AND SUMMARY

The main results of this experiment are illustrated in Fig. 1. The decay  $\gamma$  rays from the 1.99-, 3.87-, and 4.76-MeV levels of  $\text{Ne}^{24}$  are reported for the first time,

and  $\gamma$ -ray branching ratios have been determined for these levels. The 1.99- and 3.87-MeV levels have  $J=2$ . Either  $J=0$  or 1 is preferred for the 4.76-MeV level, with  $J=2$  not entirely eliminated. These results require an assumption of  $J=0$  for the ground state of  $\text{Ne}^{24}$ . Since  $T=2$  for  $\text{Ne}^{24}$ , and according to the shell model in  $jj$  coupling, the neutron  $d_{5/2}$  subshell is closed in  $\text{Ne}^{24}$ , one might expect the low-lying states in  $\text{Ne}^{24}$  to be fairly well described by  $jj$  coupling configurations involving two protons in the  $1d_{5/2}$  and  $2s_{1/2}$  orbits. (This picture has been applied to  $\text{O}^{18}$ , where two neutrons outside the  $\text{O}^{16}$  nucleus are in the  $d_{5/2}$  and  $2s_{1/2}$  orbits.<sup>13</sup>) The states which may be formed with these configurations are  $d_{5/2}^2$  ( $J^\pi=0^+, 2^+, 4^+$ ),  $s_{1/2}^2$  ( $J^\pi=0^+$ ), and  $d_{5/2}s_{1/2}$  ( $J=2^+, 3^+$ ). Of these six states, five may readily be identified with the ground and first four excited states of  $\text{O}^{18}$ . We note that there is a similarity in excitation energy between these  $\text{O}^{18}$  levels and the first few levels in  $\text{Ne}^{24}$ . If the 3.87- and 4.76-MeV levels in  $\text{Ne}^{24}$  are described by these configurations, the most reasonable assignment for the 4.76-MeV level is obtained with  $J^\pi=0^+$ . A more detailed attempt to identify the  $\text{Ne}^{24}$  levels with the appropriate shell-model configurations must await more experimental evidence.

<sup>13</sup> I. Talmi and I. Unna, Nucl. Phys. **39**, 280 (1962).

### Direct Neutron Capture in $\text{Co}^{59}(n, \gamma)\text{Co}^{60}\dagger$

O. A. WASSON, R. E. CHRIEN, M. R. BHAT, M. A. LONE,\* AND M. BEER

Brookhaven National Laboratory, Upton, New York 11973

(Received 12 August 1968)

The variation in intensity of 40 individual  $\gamma$  rays produced by neutron capture in cobalt was observed for neutron energies less than 1500 eV. The observed variations were consistent with the existence of a direct component in the radiative capture reaction mechanism. A direct-capture cross section of  $9.2 \pm 2.4$  mb at 1-eV neutron energy was deduced for the 7.492-MeV ground-state transition.

#### INTRODUCTION

EVIDENCE for the existence of a direct-reaction mechanism in the radiative capture of slow neutrons in the target nucleus  $\text{Co}^{59}$  was given in a previous article.<sup>1</sup> The present article gives more complete results, including a comparison of the  $\gamma$ -ray spectra obtained for thermal neutron capture with that from the 132-eV resonance as well as a measure of the variation in intensity of 40  $\gamma$  rays in the neutron-energy region below 1500 eV. The present experiment used a thinner cobalt sample, a smaller Ge(Li) detector, improved detector shielding from neutrons scattered by the sample, and obtained better statistical accuracy.

<sup>†</sup> This work was supported by the U. S. Atomic Energy Commission.

\* Present address: Chalk River National Laboratories, Atomic Energy of Canada, Ltd.

<sup>1</sup> O. A. Wasson, M. R. Bhat, R. E. Chrien, M. A. Lone, and M. Beer, Phys. Rev. Letters **17**, 1220 (1966).

Within the statistical accuracy, the previous results were verified.

Studies of the  $\gamma$ -ray spectrum from the  $\text{Co}^{59}(n, \gamma)\text{Co}^{60}$  reaction using thermal neutrons were reported by numerous authors.<sup>2-7</sup> The most recent measurements using Ge(Li)  $\gamma$ -ray detectors were done by Shera and Hafemeister<sup>6</sup> and by Prestwich, Kennett, and Hughes.<sup>7</sup> Shera and Hafemeister used  $\gamma$ - $\gamma$  coincidence measurements to deduce some final-state spin assignments

<sup>2</sup> G. A. Bartholomew and B. B. Kinsey, Phys. Rev. **89**, 386 (1953).

<sup>3</sup> L. V. Groshev, A. M. Demidov, V. N. Lutsenko, and V. I. Pelekhov, At. Energ. **3**, 187 (1957).

<sup>4</sup> O. A. Wasson, K. J. Wetzel, and C. K. Bockelman, Phys. Rev. **136**, B1640 (1964).

<sup>5</sup> H. U. Gersch, W. Rudolf, and K. F. Alexander, Nucl. Phys. **54**, 405 (1964).

<sup>6</sup> E. B. Shera and D. W. Hafemeister, Phys. Rev. **150**, 894 (1966).

<sup>7</sup> W. V. Prestwich, T. J. Kennett, and L. B. Hughes, Nucl. Phys. **88**, 548 (1966).

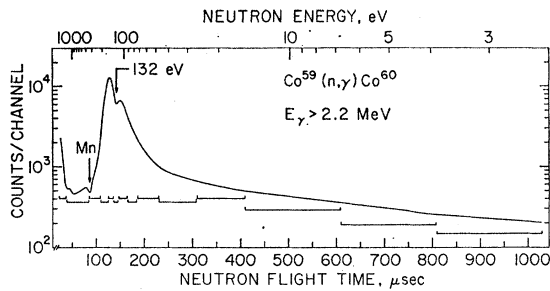


FIG. 1. Neutron time-of-flight spectrum. The horizontal bars indicate the neutron energy intervals used to obtain  $\gamma$ -ray spectra.

while three of the other experiments compared the reduced  $\gamma$ -ray transition probabilities with the corresponding reduced neutron widths of the final states populated in the  $(d, p)$  experiments of Enge, Jarrell, and Angleman.<sup>8</sup> Prestwich *et al.*<sup>7</sup> observed that the average reduced  $\gamma$ -ray intensities,  $\langle I_\gamma/E_\gamma^3 \rangle$ , for transitions to final states with  $l_n=1$  stripping patterns were approximately six times as strong as those to states showing  $l_n=3$  patterns. This was evidence for the existence of the channel resonance contribution to the capture cross section as was proposed by Lane and Lynn.<sup>9,10</sup> On the other hand, Gersch *et al.*,<sup>5</sup> who observed strong transitions to states near 2-MeV excitation energy showing weak  $(d, p)$  strengths, proposed that these states have collective character.

A comparison of the  $\gamma$ -ray spectra from capture of thermal neutrons with that from capture in the 132-eV resonance was made by Jain *et al.*,<sup>11</sup> Wasson and Draper,<sup>12</sup> and more recently by Prestwich and Coté.<sup>13</sup> The latter authors observed a negligible ( $-0.043$ ) correlation coefficient between the reduced  $\gamma$ -ray widths of the 132-eV resonance and  $(d, p)$  widths to those final states populated by  $l_n=1$  transitions in the  $(d, p)$  reaction, although the simple channel-capture model<sup>14</sup> predicts a large correlation coefficient. This lack of correlation was attributed to a lack of knowledge of the level spins and to spin-orbit splitting of the  $2p$  single-particle neutron state.

#### EXPERIMENTAL DETAILS

The cobalt sample was placed at the 22-m flight path of the fast-chopper facility<sup>15</sup> of the High Flux Beam Reactor at Brookhaven National Laboratory. The sample consisted of 392 gm of cobalt metal of 99.8% purity in sheets of size 10 cm by 14 cm. The incident

<sup>8</sup> H. A. Enge, D. L. Jarrell, and C. C. Angleman, Phys. Rev. **119**, 735 (1960).

<sup>9</sup> A. M. Lane and J. E. Lynn, Nucl. Phys. **17**, 563 (1960).

<sup>10</sup> A. M. Lane and J. E. Lynn, Nucl. Phys. **17**, 586 (1960).

<sup>11</sup> A. P. Jain, R. E. Chrien, J. A. Moore, and H. Palevsky, Nucl. Sci. Eng. **17**, 319 (1963).

<sup>12</sup> O. A. Wasson and J. E. Draper, Nucl. Phys. **78**, 576 (1966).

<sup>13</sup> W. V. Prestwich and R. E. Coté, Phys. Rev. **155**, 1223 (1967).

<sup>14</sup> C. K. Bockelman, Nucl. Phys. **13**, 205 (1959).

<sup>15</sup> R. E. Chrien and M. Reich, Nucl. Instr. Methods **53**, 93 (1967).

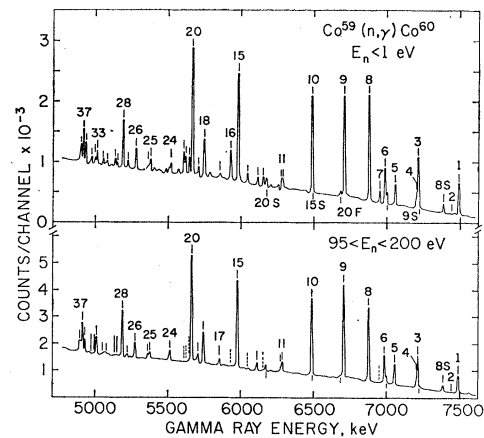


FIG. 2.  $\gamma$ -ray spectra for thermal neutron capture ( $E_n < 1$  eV) and 132-eV resonance capture. The dashed vertical lines indicate the thermal  $\gamma$  rays which are not observed in the resonance. The one-photon-escape and full-energy peaks are labeled by  $S$  and  $F$ .

neutron energies were determined by the time-of-flight technique, while the  $\gamma$  rays were detected in a 4 cm<sup>3</sup> Ge(Li) diode. The time and amplitude of each event from the  $\gamma$ -ray detector were recorded on magnetic tape and subsequently analyzed at the central computer facility.<sup>16</sup> The Ge detector was shielded from the neutrons scattered from the sample by means of 0.30 cm of lead, 0.6 cm of Li<sup>6</sup>, 5.0 cm of polyethylene, and 5.0 cm of  $(\text{Li}^6)_2(\text{CO}_3)_3$ .

At 10 000 rpm the chopper produced a neutron beam width of 7.5  $\mu\text{sec}$ , which yielded a neutron energy resolution of 0.34  $\mu\text{sec}/\text{m}$ . Six days were devoted to collecting data with the cobalt sample in the beam while one additional day was spent on background measurements. Double  $RC$  differentiation with a 2- $\mu\text{sec}$  time constant was used in the main amplifier to eliminate the flight-time-dependent gain shifts. The resultant  $\gamma$ -ray energy resolution was 9.0 keV full width at half-maximum (FWHM) at 7 MeV. The chopper speed was reduced to 1500 rpm in order to obtain a thermal spectrum.

#### THERMAL AND RESONANCE RESULTS

A neutron time-of-flight spectrum obtained for  $\gamma$ -ray events which deposited more than 2.2 MeV of energy in the Ge(Li) detector is shown in Fig. 1. The spectrum shape near the 132 eV resonance is caused by multiple scattering followed by capture in the thick ( $\frac{1}{8}$  in.) sample. The dip near 335 eV is present in the incident beam, and is probably due to manganese. The horizontal lines under the curve indicate the neutron energy intervals used to obtain  $\gamma$ -ray spectra.

The  $\gamma$ -ray spectra obtained from thermal ( $E_n < 1$  eV) neutron capture and capture in the 132-eV resonance are given in Fig. 2. The numbered peaks are the two-

<sup>16</sup> M. R. Bhat, B. R. Borrill, R. E. Chrien, S. Rankowitz, B. Soucek, and O. A. Wasson, Nucl. Instr. Methods **53**, 108 (1967).

TABLE I. Cobalt  $\gamma$ -ray energies and intensities for thermal and 132-eV resonance capture.

Peak No.	$E_\gamma$ , keV <sup>a</sup>	$E_X$ , keV <sup>b</sup>	$I_\gamma$ (th) photons/(1000 captures)	$I_\gamma$ (res)	$I_\gamma$ (th)/ $I_\gamma$ (res)	
					Present exp.	Prestwich and Coté <sup>c</sup>
1	7491.7	0	33.8±1.3	20.6±1.0	1.64±0.10	0.95
2	7432.2 <sup>d</sup>	57.5 <sup>d</sup>	<1.1	<0.7		
3	7215.6	276.1	56.0±2.2	33.2±1.5	1.68±0.10	} 1.30
4	7204.6	287.1	12.7±1.0	5.1±0.6	2.49±0.35	
5	7056.4	435.3	17.5±1.2	22.5±0.9	0.78±0.06	0.76
6	6985.9	505.8	30.0±1.6	31.8±1.0	0.95±0.06	0.94
7	6948.7	543.0	7.1±1.5	0.9±0.9	(>7)	1.62
8	6877.1	614.6	81.5±2.5	81.5±1.0	1.00±0.03	0.94
9	6705.6	786.1	73.0±2.9	92.0±1.3	0.80±0.04	0.88
10	6486.1	1005.6	62.0±2.2	70.0±1.0	0.89±0.04	0.93
11 $\alpha$	6284.1	1207.6	5.0±0.8	7.4±0.9	0.68±0.12	} 0.70
11 $\beta$	6277.3	1214.4	6.5±0.8	4.9±0.7	1.33±0.29	
12	6149.1	1342.6	4.9±1.0	<0.8	(>6)	>5
13	6111.3	1380.3	4.7±0.8	5.5±0.9	0.85±0.20	2.42
14	6040.2	1451.5	6.0±0.8	<0.8	(>7)	
15	5975.9	1515.8	57.0±2.2	65.5±1.5	0.87±0.04	0.88
16	5925.4	1566.3	15.8±0.6	1.6±1.6	(>10)	>10
17	5851.7	1639.9	2.3±0.8	3.6±0.6	0.64±0.24	2.8
18	5742.9	1748.8	17.2±1.0	19.5±0.6	0.88±0.06	0.96
19	5705.1	1786.6	3.7±0.6	5.4±0.9	0.69±0.17	1.4
20	5660.7	1831.0	60.0±2.0	69.0±1.1	0.87±0.03	0.82
21	5639.6	1852.1	7.3±0.9	2.2±1.0	3.3 ±1.5	2.3
22	5614.9	1876.8	7.0±1.4	<0.6	(>11)	5
23	5602.1	1888.6	9.0±1.4	<0.6	(>15)	5
24	5511.5	1980.2	3.4±0.5	6.0±0.4	0.57±0.10	1.25
25 $\alpha$	5372.5	2119.2	4.4±1.0	3.4±0.9	1.29±0.36	} 0.77
25 $\beta$	5360.5	2131.2	2.1±0.7	2.5±0.9	0.85±0.40	
26	5272.5	2219.2	8.9±0.7	8.4±0.4	1.06±0.09	0.7
27	5215.0	2276.7	4.1±1.0	2.7±0.9	1.52±0.30	
28	5183.9	2307.8	21.0±1.3	27.0±0.7	0.78±0.08	0.91
29	5145.3	2346.4	2.0±1.1	1.6±1.2	1.3 ±1.1	>2.5
30	5129.9	2361.8	4.5±1.5	1.2±0.8	3.7 ±2.8	
31	5066.0	2445.7	2.6±1.0	2.3±0.7	1.13±0.55	
32	5043.2	2458.5	3.0±0.8	<1.0	(>3.0)	
33	5003.6	2488.1	5.1±0.6	9.2±0.6	0.55±0.08	
34	4964.5	2527.1	2.0±1.0	1.0±1.0	(>2.0)	
35	4948.5	2543.2	2.4±1.2	<1.0	(>2.4)	
36	4922.7	2569.0	6.8±1.0	6.6±0.6	1.03±0.20	
37	4906.6	2585.1	12.3±1.0	16.0±0.6	0.77±0.07	
38 $\alpha$	4894.5	2597.2	4.9±1.0	5.8±0.6	0.85±0.19	
38 $\beta$	4884.9	2606.8	4.5±1.0	5.7±0.5	0.79±0.19	

<sup>a</sup> ±2.0 keV.  
<sup>b</sup> ±1.0 keV.  
<sup>c</sup> Taken from Ref. 13.  
<sup>d</sup> Taken from Ref. 6.

photon escape peaks following pair-production events in the Ge(Li) detector. The energy scale refers to the incident  $\gamma$ -ray energy. The peaks labeled *S* and *F* are single escape and total absorption peaks, respectively. The peak numbering system was chosen to agree with that of Shera and Hafemeister.<sup>6</sup> The dashed vertical lines in the resonance spectrum indicate the position of those  $\gamma$  rays which were observed only in the thermal spectrum.

The resulting  $\gamma$ -ray energies and intensities for the two spectra are listed in Table I. The listed excitation energies of the final states result from assuming that each  $\gamma$  ray is a primary transition from the capturing state. The errors in the  $\gamma$ -ray energies and intensities include only the statistical error in determining the  $\gamma$ -ray peak positions and net areas. The variation in  $\gamma$ -ray intensity between thermal energies and the 132-eV resonance is shown in column 6. The results of Prestwich and Coté<sup>13</sup> are listed in column 7. Unfortunately, no errors were listed by these authors; thus

the significance of the large variation in the two experiments for approximately seven of the  $\gamma$  rays is difficult to assess. It must be pointed out, however, that the statistical accuracy of the present results is superior to that of Prestwich, as a comparison of the published spectra will show.

The absolute  $\gamma$ -ray intensities were determined by normalizing the relative thermal intensities observed in this experiment to the thermal intensities measured by Shera and Hafemeister.<sup>6</sup> The  $\gamma$ -ray intensities,  $I_\gamma$ , were determined from the experimental peak areas,  $A_\gamma$ , from the expression

$$I_\gamma = kA_\gamma / \epsilon_\gamma T,$$

where  $T$  is the total counts in the  $\gamma$ -ray spectrum for  $E_c > 2.2$  MeV,  $\epsilon_\gamma$  is the relative detector efficiency, and  $k$  is a constant independent of neutron energy. It is assumed that the quantity  $T$  is a measure of the number of neutrons captured. The net peak areas were determined from a least squares fit of a Gaussian peak shape

TABLE II. Comparison of thermal γ-ray energies and intensities [units for γ-ray energies and intensities are keV and photons/(1000 captures), respectively].

Peak No.	Present work		$E_\gamma^a$	$I_\gamma^a$	$E_\gamma^b$	$I_\gamma^b$
	$E_\gamma$	$I_\gamma$				
1	7491.7±2.0	33.8±1.2	7489.7±3.0	30.0± 5.0	7495±5	26.0
2		<1.1	7432.2	1.4± 0.5		
3	7215.6	56.0±2.2	7213.7	38.0± 6.4	7218	38.0
4	7204.6	12.7±1.0	7201.6	11.0± 3.6		
5	7056.4	17.5±1.2	7055.4	16.0± 2.7	7059	15.0
6	6985.9	30.0±1.6	6984.6	30.0± 5.1	6990	25.0
7	6948.7	7.1±1.5	6949.2	6.2± 1.8	6954	5.0
8	6877.1	81.5±2.5	6876.6	85.0±14	6881	70.0
9	6705.6	73.0±2.9	6705.1	85.0±14	6710	61.0
10	6486.1	62.0±2.2	6485.3	71.0±11.6	6490	54.0
11a	6284.1	5.0±0.8	}6278.2	12.6± 2.6	6278	8.5
11b	6277.3	6.5±0.8			6177	2.5
12	6149.1	4.9±1.0	6148.9	3.7± 0.9	6152	4.5
13	6111.3	4.7±0.8	6111.0	5.0± 1.3	6112	3.8
14	6040.2	6.0±0.8	6040.9	5.9± 1.5	6045	3.8
15	5975.9	57.0±2.2	5976.0	73.0±12.0	5981	54.0
16	5925.4	15.8±0.6	5925.8	17.0±33	5927	15.0
17	5851.7	2.3±0.6	5852.4	2.3± 0.68	5851	2.5
					5782	1.0
18	5742.9	17.2±1.0	5743.3	23.0± 4.2	5744	15.0
19	5705.1	3.7±0.6	5705.1	3.6± 1.0	5705	1.0
20	5660.7	60.0±2.0	5662.0	69.0±11	5663	54.0
21	5639.6	7.3±0.9	5640.1	14.1± 3.8	5643	10.0
22	5614.9	7.0±1.4	5617.1	11.7± 3.4	}5608	13.0
23	5602.1	9.0±1.4	5604.6	15.0± 3.9		
24	5511.5	3.4±0.5	5512.6	8.7± 2.2	5512	4.5
					5444±5	2.3
25a	5372.5	4.4±1.0	}5366.4	10.2± 2.4	5411	1.5
25b	5360.5	2.1±0.7			5365	4.5
26	5272.5	8.9±0.7	5272.1	11.5± 1.9	5273	8.0
					5249	1.3
27	5215.0	4.1±1.0	5213.7	5.2± 1.3	5217	2.8
28	5183.9	21.0±1.3	5182.7	36.0± 5.9	5184	18.0
29	5145.3	2.0±1.1	5151.2	3.3± 1.0		
30	5129.9	4.5±1.5	5129.3	6.6± 1.4	5131	3.0
					5104	1.0
31	5066.0	2.6±1.0	5069.1	5.0± 1.3	5071	2.0
32	5043.2	3.0±0.8	5041.2	3.0± 0.88	5041	2.0
33	5003.6	5.1±0.6	5003.2	8.8± 1.6	5007	5.3
34	4964.5	2.0±1.0	4963.7	2.6± 1.0	4958	1.3
35	4948.5	2.4±1.2	4946.1	6.9± 2.0		
36	4922.7	6.8±1.0	4922.2	9.7± 2.5	4924	6.5
37	4906.6	12.3±1.0	4906.3	21.0± 3.9	4908	11.0
38a	4894.5	4.9±1.0	}4885.7	17.0± 4.2	4890	9.0
38b	4884.9	4.5±1.0				

<sup>a</sup> Reference 6.  
<sup>b</sup> Reference 7.

with a linear background for each γ ray. The detector efficiency was determined from the thermal neutron capture γ-ray spectrum of a natural chromium sample using the chromium absolute γ-ray intensities measured by Kane and Marriscotti.<sup>17</sup> The value of the constant  $k$  was determined by normalizing the sum of intensities of the 10 highest energy γ rays in thermal capture to the value of 373.6 photons per 1000 neutrons captured as measured by Shera and Hafemeister.<sup>6</sup>

The cobalt γ-ray energies were determined from a thermal-capture γ-ray spectrum from a composite sample of cobalt and carbon tetrachloride. The chlorine γ rays at 7790.0 keV and 6111.1 keV as measured by Rasmussen *et al.*<sup>18</sup> were used as energy standards.

<sup>17</sup> W. R. Kane and M. A. Marriscotti, Nucl. Instr. Methods **56**, 189 (1967).

<sup>18</sup> N. C. Rasmussen, Y. Hukai, T. Inouye, and V. J. Orphan, Report No. MITNE-85 1968 (unpublished).

The γ-ray energies and intensities observed in thermal capture in this experiment are compared with the results of Shera and Hafemeister<sup>6</sup> and Prestwich *et al.*<sup>7</sup> in Table II. Except for peak 29, the γ-ray energies of the present experiment agree within 3 keV with the values of Shera and Hafemeister. Except for peak 3 the γ-ray intensities agree within 20%. The γ rays at 6177, 5782, 5444, and 5411 keV observed by Prestwich *et al.* were not observed in either the present experiment or the work of Shera and Hafemeister. These peaks may result from misinterpretation of single escape peaks of lower energy γ rays. With the above exceptions the three experiments have observed the same γ rays. For this experiment, the observed double escape peak areas were corrected for contributions from single escape or full energy peaks of lower-energy γ rays whenever these latter peaks were located near the

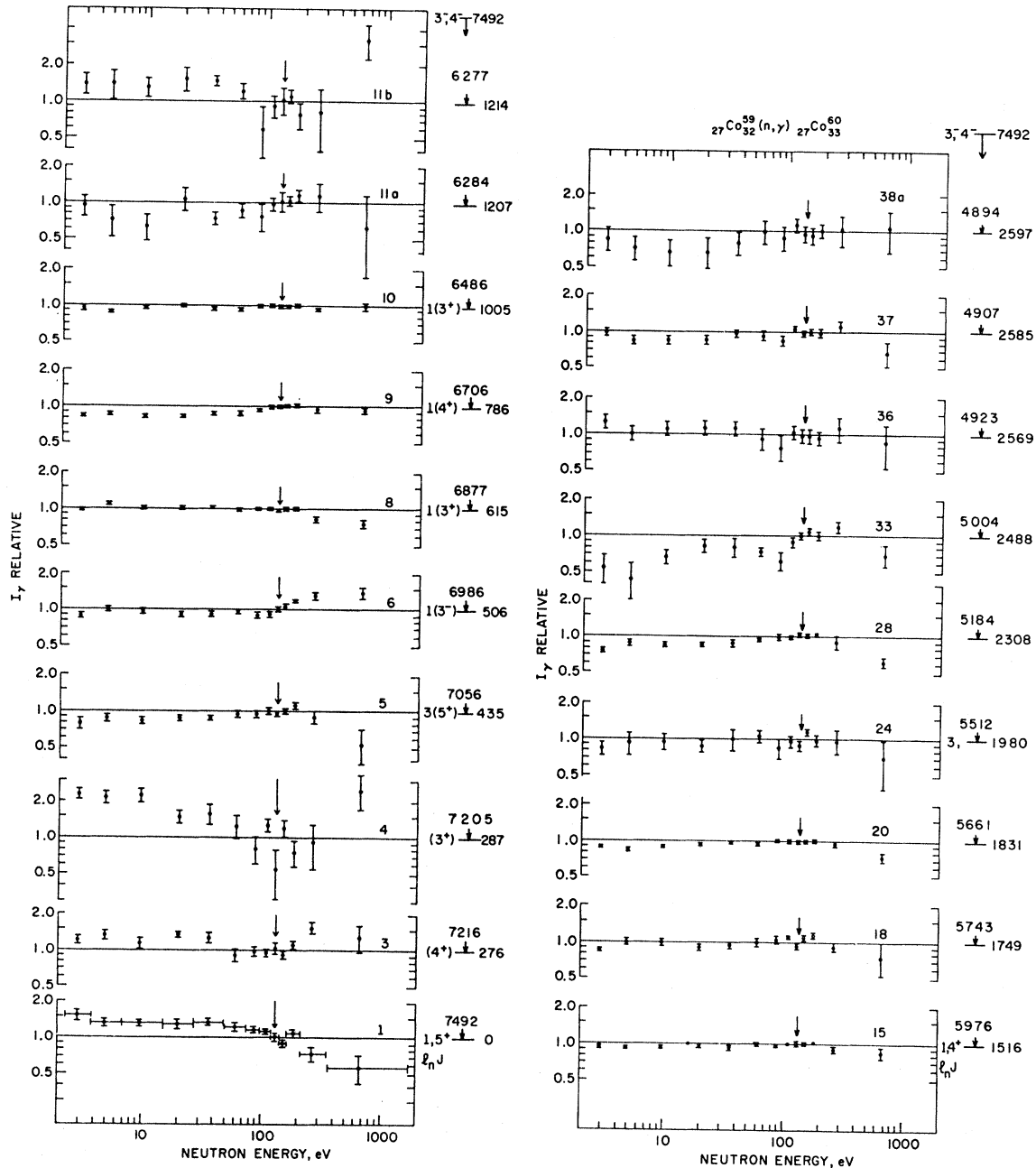


FIG. 3. Relative  $\gamma$ -ray intensity as a function of neutron energy. The neutron energy interval for each data point is indicated for peak 1. The vertical arrow indicates the 132-eV resonance. Each  $\gamma$ -ray intensity is arbitrarily normalized to unity in the 132-eV resonance. The  $\gamma$ -ray energy, excitation energy, proposed spin, and angular momentum of captured neutron in the  $(d,p)$  reaction are shown to the right of the corresponding  $\gamma$ -ray intensity.

double escape peak. The complex peaks numbered 11 and 25, which were listed as complex peaks by Shera and Hafemeister, have been fitted as doublets although the resolution was not sufficient to eliminate a more complex structure.

As is indicated by the dashed vertical lines in Fig. 2, seven of weaker  $\gamma$  rays observed in the thermal-capture spectrum are not seen in the resonance spectrum. *S*-wave neutron capture in cobalt produces resonance

spins of  $3^-$  or  $4^-$ . As was shown by Schermer,<sup>19</sup> both resonance spin states contribute to thermal capture with the  $J^\pi=4^-$  resonance at 132 eV contributing approximately 75% of the thermal-capture cross section. Assuming all observed  $\gamma$  rays to be *E1* transitions means that transitions to  $2^+$  final states are allowed for thermal capture but not for capture in the 132-eV

<sup>19</sup> R. I. Schermer, Phys. Rev. **130**, 1907 (1963).

resonance. It is thus suggested that the above 7 γ rays result from primary E1 transitions to 2<sup>+</sup> final states, although because of the wide fluctuation<sup>20</sup> of partial radiation widths, no definite spin assignments can be made for these γ rays. However, the γ-ray intensity variation between thermal and resonance capture is consistent with the final-state spin assignments proposed by Shera and Hafemeister.<sup>6</sup>

### OFF-RESONANCE RESULTS

The variation in intensity for all 40 γ rays listed in Table I was observed for neutron energies in the interval  $2 < E_n < 1800$  eV. The intensity variation for 19 of the more intense γ rays is shown in Fig. 3. The 7 γ rays with unobservable intensities in the 132-eV resonance as well as the 14 γ rays with poor statistics are excluded. Each intensity is arbitrarily normalized to unity at 132 eV. The neutron energy interval used to obtain each point is indicated by the horizontal bars for peak No. 1 as well as in Fig. 1. The position of the 132-eV resonance is indicated by the arrow. The γ-ray energy, excitation energy of final state, spin and parities of final states, and orbital angular momentum of neutrons captured in the (d, p) experiment are listed beside each intensity curve. The solid horizontal line with unit intensity is for reference only. The vertical error bars indicate the statistical standard deviations.

The relative γ-ray intensities were determined from the observed areas of the γ-ray peaks as described above. The background contribution to the total counts in each γ-ray spectrum for  $E_e > 2.2$  MeV was determined from the following measurements:

- 1 Cobalt sample with and without tungsten and manganese filters in the neutron beam;
- 2 Lead sample with and without tungsten and manganese filters in the beam; and
- 3 No sample in the beam.

The filters absorbed the incident beam near the 4.2-, 21.2-, and 337-eV resonances in tungsten and manganese. The background contribution to the observed total γ-ray spectrum was determined to be 10% at 350 eV, 6% at 2 eV, and <1% for the region of the 132-eV resonance.

In Fig. 3 the largest γ-ray intensity variations are observed for peak Nos. 1, 4, 9, and 33. The remaining γ-ray intensity variations, although significant, are less than 20% for neutron energies less than 200 eV. In our previous paper,<sup>1</sup> the intensity variation of peak 1 was attributed to interference between a direct component and the 132 eV resonance component in the partial-capture cross section which yielded a direct-capture cross section of  $9.2 \pm 2.4$  mb at 1 eV. The direct-capture contribution to the intensity variation of peaks 4, 9, and 33 was undetermined because of the unknown value of the partial radiation widths of the

TABLE III. Contribution of various resonances to the thermal-capture cross section.<sup>a</sup>

Source	$\sigma_{n\gamma}(b)$
A. Experimental	
Total	$37.2 \pm 0.6$
J=4 <sup>-</sup>	$29.0 \pm 0.5$
J=3 <sup>-</sup>	$8.2 \pm 0.5$
B. Resonances	
132-eV 4 <sup>-</sup>	$26.4 \pm 2.9$
4322-eV 4 <sup>-</sup>	0.1
5015-eV 3 <sup>-</sup>	0.3
Bound 3 <sup>-</sup>	$7.9 \pm 0.5$
Bound 4 <sup>-</sup>	$2.5 \pm 2.9$

<sup>a</sup> Deduced from Refs. 19 and 22.

3<sup>-</sup> bound level which contributed to these γ rays but not to the ground-state transition.

For S-wave neutron capture the direct radiative reaction should populate only those final states which have large admixtures of single-particle p states. The direct-capture cross section for γ-ray emission to a given final state, j, is expected to be proportional to the reduced neutron width of that state.<sup>9,10,14</sup> The direct-capture cross section is deduced from the observed γ-ray intensities  $I_j$  by means of the expression

$$I_j = \sigma_{n\gamma j} / \sigma_{n\gamma},$$

where  $\sigma_{n\gamma} = \sum_j \sigma_{n\gamma j}$  is the total-capture cross section. It is assumed that the partial-capture cross section contains a direct interaction amplitude,  $A_j$ , which interferes with the resonance amplitudes according to the form

$$\sigma_{n\gamma j} = \pi(\lambda\lambda^0) \sum_J g(J) |A_j^0 + \sum_{\lambda} (\Gamma_{\lambda n^0} \Gamma_{\lambda \gamma j})^{1/2} / (E_{\lambda} - E - \frac{1}{2}i\Gamma_{\lambda})|^2,$$

where the index 0 means evaluation at 1 eV. The resonance spins are given by J; the statistical weight factor is given by g(J); λ indicates the incident neutron wave length; the various nearby capturing states of the same J are labeled by λ; and  $\Gamma_{\lambda n^0}$ ,  $\Gamma_{\lambda \gamma j}$ ,  $\Gamma_{\lambda}$ , and  $E_{\lambda}$  refer respectively to the reduced neutron width, partial radiation width, total width, and resonance energy of capturing state λ. For cobalt the resonance spins are 3 or 4. It is further assumed that the interference terms which are present in the partial-capture cross section sum to zero in the total-capture cross section. In addition to the interference terms resulting from the direct amplitude and the resonance amplitudes, the nearby resonances of the same spin also interfere as was demonstrated by Coté and Bollinger.<sup>21</sup>

In order to evaluate the direct-capture cross section for individual γ rays in cobalt, the contribution of all the resonance amplitudes to the neutron energy region below ~500 eV is required. The contribution of the unbound levels to the total-capture cross section is

<sup>21</sup> R. E. Coté and L. M. Bollinger, Phys. Rev. Letters 6, 695 (1961).

<sup>20</sup> C. E. Porter and R. G. Thomas, Phys. Rev. 104, 483 (1956).

TABLE IV. Resonance parameters used in data analysis.

$J$	$E_r(\text{eV})$	$(g\Gamma_n^0)^{1/2}(\text{eV}^{1/2})$	$\Gamma_\gamma^{1/2}(\text{eV}^{1/2})$	$\Gamma_{\gamma j}^{1/2}(\text{eV}^{1/2})$		
				Peak 1	Peak 4	Peak 5
4	132	0.50	0.67	+0.092	+0.048	+0.097
4	4322	0.97	0.67	-0.092	+0.050	-0.060
3	-268	0.55	0.67	0	-0.050	0
3	5015	2.00	0.67	0	+0.050	0

determined from the measured resonance parameters while the bound-level contribution is determined from the fraction of the measured thermal-capture cross section which is not due to the positive energy resonances.

The thermal neutron capture cross section of cobalt<sup>22</sup> is  $37.2 \pm 0.6$  b. The contributions of the various known resonances to this cross section are listed in Table III along with the deduced bound-level contributions. According to the transmission experiments of Schermer<sup>19</sup> using polarized neutrons on a polarized target,  $21.7 \pm 1.0\%$  of the thermal-capture cross section is due to  $J=3^-$  states while the remainder is due to  $J=4^-$  states. Using the recommended resonance parameters,<sup>22</sup> the nearest positive energy  $J=4^-$  resonance at 132 eV contributes  $26.4 \pm 2.9$  b to the thermal-capture cross section while the remaining  $J=4^-$  positive energy resonances contribute  $< 0.2$  b. Thus, the  $J^\pi=4^-$  bound levels contribute no more than  $2.5 \pm 2.9$  b. The large error is due to the uncertainty in the total radiation width of the 132-eV resonance. Almost all of the  $J=3^-$  contribution is due to bound levels. Since the average level spacing near the neutron binding energy is  $\sim 1100$  eV,<sup>23</sup> it may be assumed that the  $J=3^-$  bound-level contribution is due to a single level.

Since the ground-state spin and parity of Co<sup>60</sup> is  $5^+$ , electric dipole transitions to this state are possible only for the  $J=4$  capturing states. For this case, the  $J=3$  resonances only contribute to the total-capture cross section, resulting in a straightforward evaluation of the  $\gamma$ -ray intensity variation. The effect of a direct-capture cross section of 9.2 mb at 1 eV is shown in Fig. 4. The upper curve results from constructive interference at 1 eV between the direct and 132-eV resonance amplitudes while the other curve results for no direct capture. The effect of the higher-energy resonances for  $E_n < 100$  eV is small but is important in the higher neutron energies. The resonance parameters used in the calculations are listed in Table IV.

As was previously shown, the  $J^\pi=4^-$  bound levels may contribute  $2.6 \pm 2.9$  b to the thermal-capture cross section. If the direct-capture cross section of 9.2 mb at 1 eV for the ground-state transition is replaced by a bound  $J^\pi=4^-$  level which contributes 2.6 b to the

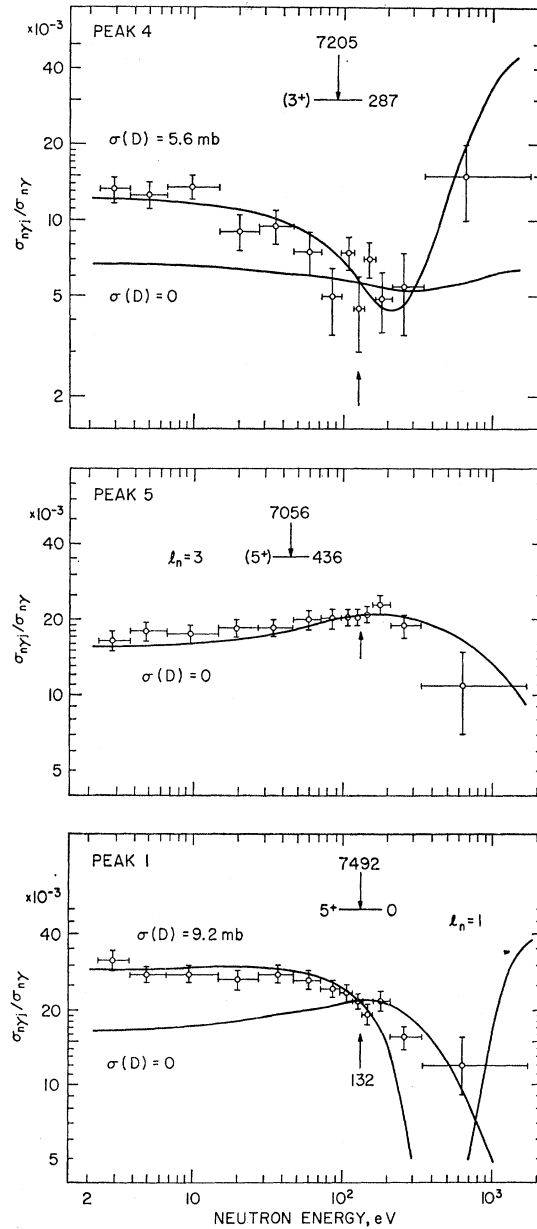


Fig. 4. Intensity variation of  $\gamma$ -ray peak Nos. 1, 4, and 5. The horizontal bars on the data points indicate the neutron energy interval, while the vertical bars indicate the statistical error. The resonance parameters used to calculate the various curves are listed in Table IV.

<sup>22</sup> M. D. Goldberg, S. F. Mughabghab, B. A. Magurno, and V. M. May, Brookhaven National Laboratory Report No. BNL-325, 1966, 2nd ed., Suppl. No. 2, Vol. IIA (unpublished).

<sup>23</sup> J. Morgenstern, S. de Barros, A. Bloch, P. L. Chevillon, V. D. Huynh, H. E. Jackson, J. Julien, C. Lopata, and C. Samour, Nucl. Phys. A102, 602 (1967).

TABLE V. Estimated values of the direct-capture cross sections assuming that  $\sigma_j(D) = b \sum_J (2J_f + 1) \theta_{N_f}^2$ , where the value of  $b$  is determined from peak 1 using the listed values of  $J_f$ . The value of  $J^\pi$  for the state populated by  $\gamma$ -ray number 21 was arbitrarily chosen to be  $3^+$ .

Peak No.	$J_f^\pi$ <sup>a</sup>	$l_n$ <sup>b</sup>	$(2J_f + 1) \theta_{N_f}^2$ <sup>b</sup>	$\sigma_j(D)$ (1 eV) (mb)	$\Gamma_{\gamma j}(132 \text{ eV})$ (meV)	$[\sigma_j(D)/\sigma(132)](1 \text{ eV})$
1	5 <sup>+</sup>	1	55	9.2	9.2	$1.1 \times 10^{-1}$
2	2 <sup>+</sup>	1	33	5.6	<0.3	<20.0
3	(4 <sup>+</sup> )	}1,(3)	21	7.0	15.0	0.50
4	(3 <sup>+</sup> )			7.0	2.3	3.2
6	(3 <sup>+</sup> )	1	17	5.7	14.3	0.43
8	(3 <sup>+</sup> )	1	31	10.3	36.6	0.30
9	(4 <sup>+</sup> )	1	22	7.3	41.4	0.19
10	(3 <sup>+</sup> )	1,(3)	47	16.0	31.5	0.55
15	(4 <sup>+</sup> )	1	6	2.0	29.5	0.07
21	(3 <sup>+</sup> )	1	5	1.7	1.0	1.8

<sup>a</sup> Reference 6.  
<sup>b</sup> Reference 8.

thermal-capture cross section, the required partial radiation width of the bound level is 11.3 meV. This is about equal to the partial radiation width of the 132 eV resonance. Thus, a bound level with  $J^\pi = 4^-$  contributing 2.6 b to the thermal-capture cross section is sufficient to simulate a direct amplitude in the region below 100 eV. Evidence that the  $J^\pi = 4^-$  bound-level contribution is not important, however, is obtained from the intensity variation of the other  $\gamma$  rays as given below.

The assumption that the 5<sup>+</sup> spin assignment is correct for the 435 keV final state populated by  $\gamma$ -ray No. 5 allows a measure of the  $J = 4$  bound-level contribution. As for the ground-state transition,  $E1$  transitions occur only from the  $J = 4$  levels for this  $\gamma$  ray. No direct capture should occur for this  $\gamma$  ray since  $l_n = 3$  in the  $d, p$  reaction and the  $p$ -wave admixture in the final state is thus small. As is shown in Fig. 4 a satisfactory fit to the data is obtained for no  $J = 4^-$  bound-level contribution and for no direct capture. The resonance parameters used in the analyses are listed in Table IV. Further calculations show that if a significant  $J = 4$  bound level exists, its partial radiation width is quite small [ $\Gamma_{\gamma j}(\text{bound}) < 0.1 \Gamma_{\gamma j}(132 \text{ eV})$ ]. However, because of the broad distribution of partial radiation widths, the failure of a  $J = 4^-$  bound level to contribute to peak No. 5 does not entirely eliminate the possibility that such a level could contribute to other  $\gamma$  rays. The strongest evidence against the existence of a bound level of sufficient strength to simulate a direct cross section is the small variation in intensity of most of the  $\gamma$  rays. Most of the  $\gamma$  rays result from capture in both 3<sup>-</sup> and 4<sup>-</sup> capturing states which makes the calculation of the resonance amplitudes uncertain since the partial radiation widths are known only for the 132-eV resonance. Calculations including a  $J^\pi = 4^-$  bound level which contributes 2.6 b to the thermal-capture cross sections as well as the 4 resonances listed in Table IV indicate that the interference between the presumed  $J = 4$  bound level and the 132-eV resonance dominates the partial-capture cross section below 100 eV. Further calculations assuming the same value of the partial

radiation width for each resonance show a variation in  $\gamma$ -ray intensity of a factor of 2 between 1 and 132 eV. The failure to observe such large variations in intensity for any of strong  $\gamma$  rays in Fig. 3 is convincing evidence that the contribution of the  $J^\pi = 4^-$  bound levels to the neutron energy region above 1 eV is small. Thus the intensity variation for the ground-state transition demonstrates the existence of a direct component in the reaction mechanism.

It is concluded that the direct-capture cross section for emission of the ground state  $\gamma$  ray is  $9.2 \pm 3.0$  mb at 1 eV where the uncertainty of  $\pm 3.0$  mb includes the errors in the partial radiation widths of the positive energy resonances.

According to Lane and Lynn,<sup>10</sup> the direct-capture process includes a contribution from hard-sphere scattering as well as a contribution from the far-away resonances. The contribution of hard-sphere scattering to the direct-capture cross section for  $s$ -wave neutron capture to populate a final state of spin,  $J_f$ , via emission of a 7.49-MeV  $\gamma$  ray is calculated from Eq. 1 of Lane and Lynn<sup>10</sup> to be

$$\sigma_j(\text{hard sphere})(1 \text{ eV}) = \sum_J \frac{(2J_f + 1)}{6(2I + 1)} 54.8 \theta_{N_f}^2 \text{ mb},$$

where the summation is over the intermediate states of spin  $J$  which can yield  $E1$  transitions to a final state,  $j$ , of spin  $J_f$  and  $\theta_{N_f}^2$ , a number less than unity, is the dimensionless reduced neutron width of the final state. For a final state of spin 5 which is populated by peak No. 1, the resulting hard-sphere contribution to the direct-capture cross section is 12.6 mb at 1 eV for  $\theta_{N_f}^2 = 1$ . The direct-capture cross section of 9.2 mb at 1 eV deduced in this experiment for the ground-state transition is consistent, within an order of magnitude, with the predictions of hard-sphere capture of Lane and Lynn.

For the remaining  $\gamma$  rays an estimate of the direct-capture cross section, including both hard-sphere scat-

tering and the contribution of distant resonances, is obtained by assuming that

$$\sigma_j(\text{direct}) = b \sum_J (2J_f + 1) \theta_{N_f}^2,$$

where the quantity  $(2J_f + 1) \theta_{N_f}^2$  is determined from the  $(d, p)$  experiments and the constant  $b$  is determined from the measured direct-capture cross section of the ground-state transition. The resulting estimates of the direct-capture cross section for those  $\gamma$  rays populating final states which yielded  $l_n = 1$   $(d, p)$  stripping patterns are given in Table V. It is assumed that all listed states have pure  $l_n = 1$  contributions and that peak Nos. 3 and 4 each have the value of the spectroscopic factor observed for the unresolved pair in the  $(d, p)$  experiment. The spin and parity of the state populated by peak No. 21 was arbitrarily assumed to be  $3^+$ . The effect of direct capture on the  $\gamma$ -ray intensity variation is determined from the magnitude of the direct-capture cross section relative to that of the 132-eV resonance. This ratio evaluated at 1 eV is indicated in column 7. Although the estimated direct-capture cross section of peak No. 10 is larger than peak No. 1, the intensity variation of peak No. 10 is less because of the larger value of the partial radiation width of peak No. 10. The results of Table V indicate that the intensity variation caused by the estimated direct capture is large for peak Nos. 1 and 4 and small for the remaining  $\gamma$  rays. The intensity of peak No. 21 is too small for quantitative analysis. The observed  $\gamma$ -ray intensity variations are consistent with the direct-capture hypothesis.

The calculated intensity variation for  $\gamma$ -ray peak No. 4 is shown in Fig. 4 for the direct-capture cross section at 1 eV equal to zero and to 5.6 mb as estimated above. The value of 5.6 mb yields an excellent fit to the data, although the uncertainty in the direct-capture cross section is undetermined due to the uncertainty in the neighboring partial radiation widths. Unlike peak No. 1, the  $J = 3$  resonances also contribute to the partial-capture cross section since the final-state spin and parity are probably  $3^+$ . It is assumed that the partial radiation widths of the 4 resonances included

in the calculation are equal to the partial radiation width of the 132 eV resonance. The resonance parameters used in the calculation are listed in Table IV. It is emphasized that although the inclusion of the estimated direct-capture cross section of 5.6 mb at 1 eV in addition to the contribution of the nearby resonances yields an excellent fit to the experimental data, the fit is not unique because only the value of the partial radiation width of the 132-eV resonance is known.

Due to the small variation in  $\gamma$ -ray intensity, no deductions of the direct-capture cross section for the remaining  $\gamma$  rays was attempted. The variations in intensity of the  $\gamma$  rays observed in this experiment are qualitatively consistent with the expectations of the direct-capture process. However, only for the ground-state transition was a definite determination of the direct-capture cross section obtained.

### SUMMARY

The experimentally observed variation in individual  $\gamma$ -ray intensities as a function of neutron energy for neutron energies less than 1 keV is consistent with the hypothesis that a direct reaction mechanism occurs in addition to the usual compound nucleus formation in the radiative capture of low-energy neutrons in cobalt. Strong evidence supports the conclusion that for the ground-state transition a direct-capture cross section of  $9.2 \pm 3.0$  mb and not a nearby bound level is the source of the  $\gamma$ -ray intensity variation. For  $\gamma$ -ray peak No. 4 a less strong determination of the direct-capture cross section is made because of the influence of the unknown partial widths of the important resonances. The observed variation in  $\gamma$ -ray intensity between thermal and the 132-eV resonance is consistent with the final-state spin assignments of Shera and Hafemeister.<sup>6</sup>

### ACKNOWLEDGMENTS

The authors thank Hobart Kraner and Marco Jamini for supplying the Ge(Li) detectors, and Fred Paffrath and Vito Manzella for maintaining the chopper and electronic equipment.